A Study on Ship Speed Loss due to Added Resistance in a Seaway

Proceedings of the Twenty-sixth (2016) International Ocean and Polar Engineering Conference **www.isope.org**
Rhodes, Greece, June 26-July 1, 2016

ISBN 978-1-880653-88-3; ISSN 1098-6189

A Study on Ship Speed Loss due to Added Resistance in a Seaway

Mingyu Kim [a,*], *Olgun Hizir* [b], *Osman Turan* [a], *Sandy Day* [a] *and Atilla Incecik* [a]
[a] Department of Naval Architecture, Ocean and Marine Engineering, University of Strathclyde, Glasgow, United Kingdom
[b] Orwell Offshore Ltd., Suffolk, United Kingdom

ABSTRACT

The accurate prediction of the added resistance with motions and the ship attainable speed under actual weather conditions is essential to evaluate the ship performance in realistic operation conditions, plan a safe and energy efficient voyage and assess environmental impact. Regarding the international regulations, the ship speed reduction coefficient (fw) due to wind and waves is under discussion in International Maritime Organization (IMO) to calculate Energy Efficiency Design Index (EEDI) for new ships in the representative sea conditions of wind and waves. In the present study, a reliable methodology is presented to estimate the added resistance and the ship speed loss of a container ship in specific sea conditions of wind and waves in random seas and the effect on the ship speed loss by the change of ship speed was investigated with consideration for the slow steaming.

KEY WORDS: *Ship speed loss; added resistance; ship motions; potential flow; computational fluid dynamics; Beaufort scale.*

INTRODUCTION

Now more than ever, reduction of ship pollution and emissions, maximization of energy efficiency, enhancement of safety requirements and minimization of operational expenditure have been required. Traditionally, ship resistance and propulsion performance in calm water has been concentrated in the ship design stage even though there have been some changes for ship and hull form design from design draught and speed to specific range of draught and speed considering operating profile (Kim and Park, 2015). When a ship advances through a seaway, she requires additional power in comparison with the power required in calm water due to actual weather, hull fouling and other operating conditions. This degradation of the ship performance in a seaway is generally called "Sea Margin" which is the percentage of the additional power needed on top of the power required the in calm water. Sea margin is reported to be about 15-30% of the power required in calm water (Arribas, 2007), whereas a 15% sea margin most commonly applied. A more accurate prediction of the added resistance with motions and ship speed loss is essential not only to assess the sea margin to determine the engine and propeller design point, but to evaluate the ship performance and environmental impact under actual weather and operating conditions.

Regarding the international regulations, the Marine Environment Protection Committee (MEPC) of the International Maritime Organization (IMO) issued environmental regulations to meet the requirements in order to improve the energy efficiency level and to reduce carbon emissions. These regulations include Energy Efficiency Design Index (EEDI) as a mandatory technical measure for new ships and Energy Efficiency Operational Indicator (EEOI) which is related to ship voyage and operational efficiency as a voluntary technical measure for ships in service. Recently, the ship speed reduction coefficient (fw) is under discussion for the calculation of EEDI in the representative sea conditions (IMO MEPC, 2012).

Meanwhile, the added resistance problem due to waves has been widely studied by conducting experiment and numerical simulations by the potential flow theory and Computational Fluid Dynamics (CFD). For potential flow methods, there are two major analytical approaches for the calculation of the added resistance using the velocity potentials; the far-field method and the near-field method. The far-field method is based on the added resistance computed from the wave energy and the momentum flux generated from a ship and is evaluated across a vertical control surface of infinite radius surrounding the ship. The first study was introduced by Maruo (1960) using Kochin function which consists of radiating and diffracting wave components and investigated in detail by Joosen (1966) and Newman (1967). Later on, the far-field method based on radiated energy approach was proposed by Gerritsma and Beukelman (1972) for added resistance in head seas and has become popular in strip theory programs due to its easy implementation. On the other hand, the near-field method estimates the added resistance by the integration of hydrodynamic pressure on the body surface, which was first introduced by Havelock (1937) where the Froude-Krylov approach was used to calculate hull pressures. Boese (1970) proposed a simplified method where the importance of relative wave height contribution to the added resistance was first addressed. The near-field method was improved by Faltinsen et al. (1980) based on the direct pressure integration approach and the 2-D linear strip theory by Salvesen et al. (1970) with the introduction of a simplified asymptotic method in short waves. Joncquez (2009) and Kim et al. (2007) solved the added resistance based on Rankine panel method using time-domain approach with B-spline functions to the added resistance problem.

Presently as computational facilities have become more powerful and more accessible, CFD techniques have been more commonly used to predict the added resistance and ship motions taking into account viscous effects and large ship motions as well as the effect of breaking waves and green water effect. Recently, Guo et al. (2012) predicted motions and the added resistance for KVLCC2 using ISIS-CFD flow solver as RANS code whilst Sadat-Hosseini et al. (2013) predicted the added resistance and motions for KVLCC2 using CFDSHIP-IOWA as Unsteady Reynolds-Averaged Navier-Stokes (URANS) code and Simonsen et al. (2013) carried out numerical simulations for the ship motions, flow field and added resistance for KCS containership using Experimental Fluid Dynamics (EFD) and CFD. Tezdogan et al. (2015) performed URANS simulations to estimate the effective power and fuel consumption of the full scale KCS containership in waves by predicted added resistance in regular head seas using a commercial CFD program, Star-CCM+. In addition to researches on accurate prediction of the added resistance and ship motions in waves, there have been studies on reduction of the added resistance by developing hull form. Park et al. (2014) modified the forebody of KVLCC2 as Ax-bow and Leadge-bow types to reduce the added resistance in waves by means of EFD and potential theories. Kim et al. (2014) revised bulbous bow of a containership to optimize hull form for both operating conditions in calm water and wave conditions by CFD simulations. Also there have been researches on the ship speed loss in a seaway (Kwon, 2008; Kashiwagi, 2009; Prpić-Oršić and Faltinsen, 2012).

In the present study, the main aim is the development of a reliable methodology to estimate the added resistance and the ship speed loss due to wind and waves. Firstly, validation studies have been conducted to calculate the added resistance with the vessel advancing in regular head and oblique waves, which is one of the major components affecting ship performance, using 2-D linearized potential flow method and CFD method. Secondly, after the validation of the added resistance in regular waves, spectral analysis is performed and the methodology is extended to calculate added resistance and ship speed loss in irregular waves using 2-D potential flow method. The added resistance due to wind and irregular waves is estimated using significant wave height, mean wave period and mean wind speed parameters corresponding to the Beaufort scale based on IMO and ITTC guideline/recommendation (IMO MEPC, 2012; 27th ITTC seakeeping committee, 2014) and results are compared with simulation results obtained by other researchers. Finally, with consideration for the slow steaming of the containership speeds (Banks et al., 2013), the effect of the ship speed loss at preliminary design and other lower speeds was investigated.

SHIP PARTICULARS AND COORDINATE SYSTEM

All calculations of the added resistance and ship speed loss have been performed for the S175 containership, which is one of benchmark hull forms to study seakeeping capability by several researchers. The main particulars of the ship are given in Table 1. For CFD simulations of the added resistance and ship motions in regular waves, the model with scale ratio of 1/40 is employed in calculations.

Table 1. Main particulars of S175 containership

Symbol	Ship
Length between perpendiculars (L_{PP})	175 m
Breadth (B)	25.4 m
Draught (T)	9.5 m
Block coefficient (C_B)	0.572
Displacement (Δ)	24,272 ton
Longitudinal centre of gravity (LCG) from aft peak	85.16 m
Vertical centre of gravity (KG)	9.52 m

In the numerical simulations, a right-handed coordinate system (x, y, z) is adopted. Fig. 1 shows the employed coordinate system where the translational displacements in the x, y and z directions are η_1(surge), η_2(sway) and η_3(heave), and the angular displacements of rotational motion about the x, y and z axes are η_4(roll), η_5(pitch) and η_6(yaw) respectively and θ angle represents the ship's heading angle to incident waves. For head seas θ angle equals 180 degree and for beam wave from port side equals 90 degrees.

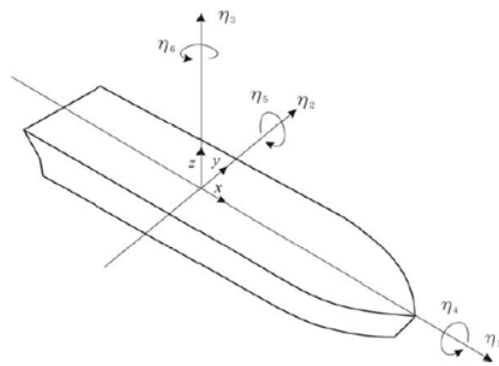

Fig. 1. Coordinate system

NUMERICAL METHODS AND MODELLING

In the present study, the 2-D linear potential method and CFD method were applied for the validation study on the added resistance and ship motions in regular waves. For the numerical calculation of the added resistance due to irregular waves, the 2-D linear potential method was used.

2-D Linear Potential Method

The calculation of the added resistance and ship motions in waves is carried out with 2-D linear potential method software ShipX. The program is developed by MARINTEK (Norwegian Marine Technology Research Institute) as common platform for ship design analysis on ship motions and global loads in early design stage based on the 2-D linear potential using the strip theory (Salvesen et al., 1970). In ShipX program, the calculation of the added resistance in waves can be performed by using two different approaches. The first approach is the far-field method based on the momentum conservation theory developed by Gerritsma and Beukelman (1972) and generalized and extended to oblique waves by Loukakis and Sclavounos (1978). The second approach is near-filed method to integrate hydrodynamics pressure on the body surface including asymptotic formula in short waves to overcome the deficiency of the approach (Faltinsen et al., 1980). In current study, the second approach is chosen for the calculation of the added resistance because the first approach shows large difference in the peak values while negative values conflict with the experimental data for the case of the following waves as shown in Fig. 2. The main reason for the poor agreement in the following seas between the far-field and experimental results is attributed to the inaccuracies in the hydrodynamic coefficients and motions in the strip theory method which assumes low Froude number, high frequency and slender body (McTaggart et al., 1997) based on the formula by Gerritsma and Beukelman. But if the original Maruo's formula combined with correct computation of the Kochin function using the strip method is applied for the following sea, a reasonable agreement with experimental data would be expected. In the current study, opposing to the strip theory Froude number is high (Fn=0.25) hence the

Pulsating Source (PS) method in the strip theory fails to satisfy the forward speed Free Surface Boundary Condition (FSBC). However, the near-field method uses the drift forces obtained by the direct pressure integration method on the hull surface where drift forces are dominated by the ship relative motion. The strip theory predicts relative motions superior to the damping coefficients therefore the near-field method agreed better with the experiments compared to the far-field method.

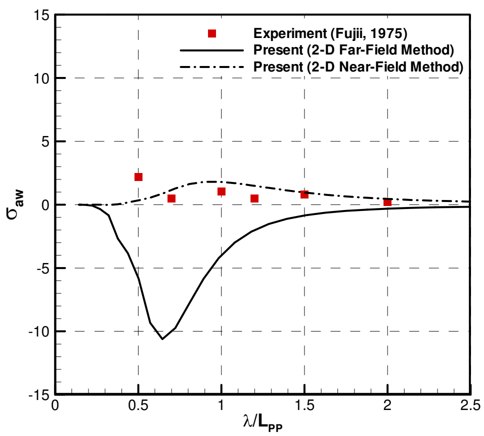

Fig. 2. Added resistance for S175 (Fn=0.25, θ=0°)

The added resistance due to waves (ΔR_{wave}) is given by Eq. 1 (Faltinsen et al., 1980)

$$\Delta R_{wave} = \int_c \left\{-\frac{\rho g}{2}\cdot\overline{\zeta_r^2}\right\} n_1 ds - \omega^2 M\overline{\eta_3\eta_5} + \omega^2 M\overline{(\eta_2 - z_G\eta_6)\eta_6}$$
$$+\rho\int_{S_B}\overline{\left\{(\eta_2 + x\eta_6 - z\eta_4)\frac{\partial}{\partial y}\left(\frac{\partial\phi^{(1)}}{\partial t} - U\frac{\partial\phi^{(1)}}{\partial x}\right)\right|_m}$$
$$\overline{+(\eta_3 - x\eta_5 + y\eta_4)\frac{\partial}{\partial z}\left(\frac{\partial\phi^{(1)}}{\partial t} - U\frac{\partial\phi^{(1)}}{\partial x}\right)\Big|_m}$$
$$\overline{+\frac{1}{2}\left(\left(\frac{\partial\phi^{(1)}}{\partial y}\right)^2 + \left(\frac{\partial\phi^{(1)}}{\partial z}\right)^2\right)}\Bigg\} n_1 ds\Bigg|_m \quad (1)$$

where $\zeta_r = \zeta - (\eta_3 - x\eta_5 + y\eta_4)$ is the relative wave amplitude along the ship and ζ is the wave elevation, c is the water line curve, ρ is the water density, g is the acceleration of gravity, n_i is the i[th] component of normal vector pointing into ship and S_B is the mean wetted surface of the vessel. M is the vessel mass and $\phi^{(1)}$ denotes the linear first order velocity potential. The bar over the expressions indicates time-averaged values, while m indicates that the variables are evaluated on the mean position of the wetted ship hull. The added resistance (ΔR_{wave}) is non-dimensionalised as follows;

$$\sigma_{aw} = \frac{\Delta R_{wave}}{\rho g A^2 B^2 / L_{PP}} \quad (2)$$

where A is wave amplitude. The added resistance of the vessel due to waves will be presented by the added resistance coefficient (σ_{aw}) over the wave/ship length ratios (λ/L_{PP}).

Computational Fluid Dynamics (CFD)

An Unsteady Reynolds-Averaged Navier-Stokes (URANS) was applied to calculate the added resistance in regular waves by the commercial CFD software STAR-CCM+. For incompressible flows, if there are no mesh motion and external force, the averaged continuity and momentum equations are given in tensor form and Cartesian coordinates by Eqs. 3~4

$$\frac{\partial(\rho\bar{u}_i)}{\partial x_i} = 0 \quad (3)$$

$$\frac{\partial(\rho\bar{u}_i)}{\partial t} + \frac{\partial}{\partial x_j}\left(\rho\bar{u}_i\bar{u}_j + \rho\overline{u_i'u_j'}\right) = -\frac{\partial\bar{p}}{\partial x_i} + \frac{\partial\bar{\tau}_{ij}}{\partial x_j} \quad (4)$$

where $\bar{u}_i$ is the averaged velocity vector of fluid, $\overline{u_i'u_j'}$ is the Reynolds stresses and $\bar{p}$ is the mean pressure. For Newtonian fluid under incompressible flow, the mean shear stress tensor, $\bar{\tau}_{ij}$, is expressed in Eq. 5 where μ stands for dynamic viscosity.

$$\bar{\tau}_{ij} = \mu\left(\frac{\partial\bar{u}_i}{\partial x_j} + \frac{\partial\bar{u}_j}{\partial x_i}\right) \quad (5)$$

The Finite Volume Method (FVM) and the Volume of Fluid (VoF) method were applied for the spatial discretization and free surface modelling individually. The flow equations were solved in a segregated manner with a predictor-corrector approach. Convection and diffusion terms in the RANS equations were discretised by a second-order upwind scheme and a central difference scheme. Semi-implicit method for pressure-linked equations (SIMPLE) algorithm was used to resolve the pressure-velocity coupling and a standard $k-\varepsilon$ model was applied as the turbulence model. In order to consider ship motions, a Dynamic Fluid Body Interaction (DFBI) scheme was applied with vessel free to move in heave and pitch directions.
The ship hull with a scale ratio of 1/40 was used. Control volume of the whole domain were taken into account with overset mesh, which is relevant to simulation of the ship with large amplitude motions in high waves and parametric studies without any conformal mesh generation, considering simulations of oblique waves for future studies. In overset mesh, flow-field information is passed between region surrounding the body of interest and background region containing the far-field flow domain. The calculation domain is applied as $-2L_{PP} < x < 1.0L_{PP}$, $-1.5L_{PP} < y < 1.5L_{PP}$, $-1.5L_{PP} < z < 1.0L_{PP}$ where the mid-plane of the ship is located at $y = 0$ and ship draught is at z= 0. . The total number of cells is in order of 4 million. Each boundary conditions with the generated mesh applied to the simulation is depicted in Fig. 3.

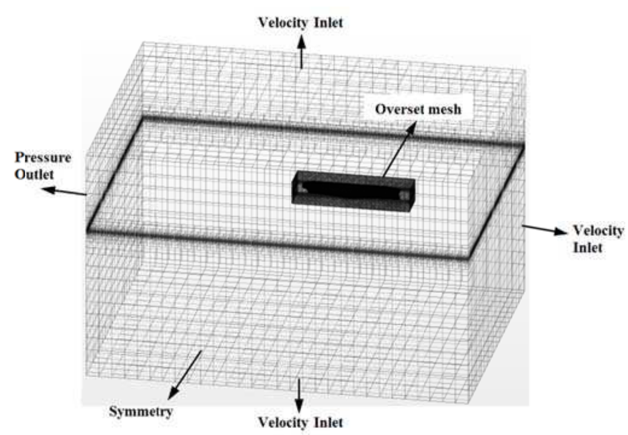

Fig. 3. Meshes and boundary conditions

The added resistance due to waves (ΔR_{wave}) is obtained by Eq. 6

$$\Delta R_{wave} = R_{wave} - R_c \quad (6)$$

where R_{wave} and R_c are resistance in wave conditions and calm water respectively, which are all predicted by CFD.
The CFD simulations including calm water condition were performed

as summarized in Table 2, each identified by their case numbers. The ratio of non-dimensionalised wave length (λ/L_{PP}) is selected between 0.5 and 1.5, and the wave steepness in all cases was chosen to be $1/60$. In all cases, the ship speed is 1.6375 m/s with Fn=0.25 which is corresponding to the ship speed of 20.14 kts. Regarding wave direction, the cases of following waves are considered for the validation of CFD simulations and the comparison with the results of 2-D potential method and experimental data.

Table 2. CFD test conditions in calm water and regular waves (Fn=0.25)

Case no. C	Wave length λ/L_{PP}	Wave height H (m)	Wave direction
0	-	-	-
1	0.50	0.03646	Head/following
2	0.70	0.05104	Head
3	0.85	0.06198	Head/following
4	1.00	0.07292	Head
5	1.15	0.08385	Head/following
6	1.30	0.09479	Head
7	1.50	0.10938	Head

Before calculating the added resistance of the ship due to waves, wave calibration test was performed for the wave conditions of the case 5 (C5) in Table 2. Fig. 4 shows the results of wave elevation in calculation domain. The difference of the simulated wave height between the inlet and ship and the input wave of the case 5 is 2% to 3.5%, which means the used cell size and time step is acceptable for the current CFD simulation model (Tezdogan et al., 2015; Kim et al. 2015).

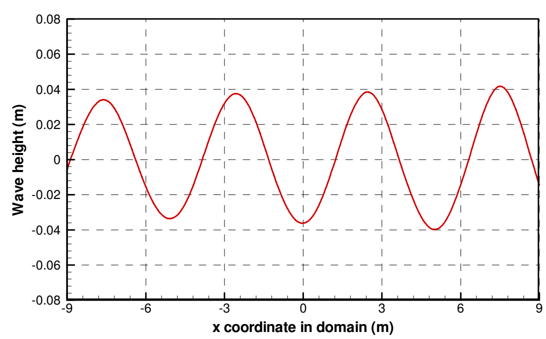

Fig. 4. Wave calibration results (wave conditions of the case 5)

ESTIMATION OF SHIP SPEED LOSS

The flowchart in Fig. 5 illustrates the procedure of the developed methodology to estimate the ship speed loss due to wind and irregular waves considering the specific sea condition. ΔR_{wave} and ΔR_{wind} are the added resistance due to wave and wind, and η_D and η_S are the propulsion and transmission efficiency respectively. The properties for propellers and propulsion efficiency η_D are estimated based on Holtrop and Mannen's method (1978, 1982 and 1984) and transmission efficiency of the ship is assumed to be 0.99.

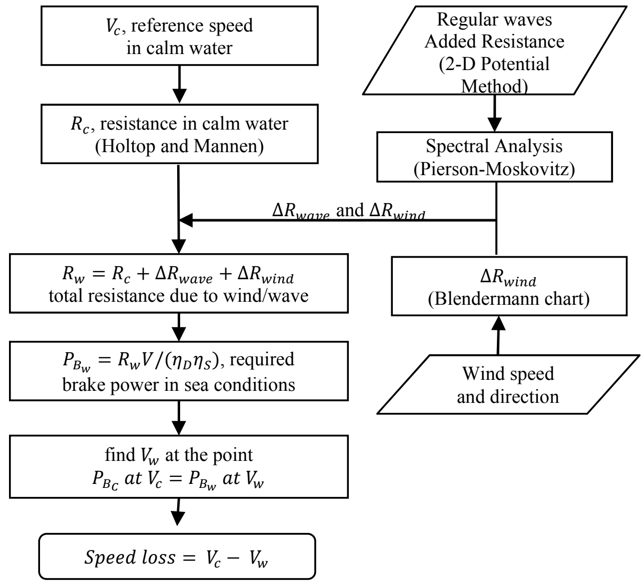

Fig. 5. Procedure of the ship speed loss estimation

Prediction of Resistance in Calm Water

Firstly the resistance and required power in calm water have to be estimated in advance. In this developed methodology, the resistance and required power are estimated based on Holtrop and Mennen's method (1978, 1982 and 1984) which is a regression approach based on model experiments and full-scale data, and a useful method for estimating resistance and propulsive powers at initial design stage with model test data for similar ships and numerical simulation results.

Added Resistance due to Waves and Wind

Regarding the numerical calculation of the added resistance due to irregular waves, the 2-D linear potential method was used. Although some of the assumptions and simplifications are applied, the linear potential theory has been found to give very good results compared to experimental data with minimal computational cost. Since the speed reduction coefficient (fw) (IMO MEPC, 2011) was introduced and adopted for the calculation of EEDI, the application procedures for the calculation of fw have been discussed in the representative sea condition of wave height, mean wave period and wind speed for the head wind and waves. As the representative sea condition, Beaufort Number (B.N.) 6 was chosen by MEPC (2012) considering mean sea conditions of north Atlantic and north Pacific. In this study, the two parameter Pierson-Moskowitz spectrum based on significant wave height (Hs) and mean wave period (Tm) in short-crested waves with cosine-squared function is used under the assumption that sea condition of interest is fully developed sea. Table 3 shows typical sea conditions corresponding Beaufort number up to 7 including the representative parameters at B.N. 6 to consider fw in EEDI formula.

The relation between B.N. and significant wave height is taken from data published by the Open University (1999) which described sea state, significant wave height and wind speed corresponding to each B.N. in fully developed sea. Also, the relation between Hs and Tm is taken from the formula which is recommended by the 27th ITTC seakeeping committee (2014) as expressed by Eq. 7.

$$T_m = 3.86\sqrt{H_S} \quad (7)$$

Table 3. Typical sea conditions corresponding Beaufort number

Beaufort number, B.N.	Mean wind speed, U_{wind} [m/s]	Significant wave height, Hs [m]	Mean wave period, Tm [s]
0	0.0	0.0	0.000
1	0.9	0.1	1.22
2	2.3	0.4	2.44
3	4.4	0.8	3.45
4	6.7	1.5	4.73
5	9.4	2.0	5.46
6	12.6	3.0	6.67
7	15.5	4.5	8.19

The added resistance (ΔR_{wind}) due to wind was calculated by Eq. 8 (IMO MEPC, 2012)

$$\Delta R_{wind} = \frac{1}{2}\rho_a A_T C_{D_{wind}} \left\{(U_{wind} + V_w)^2 - V^2{}_c\right\} \quad (8)$$

where ρ_a is density of air, A_T is the frontal projected area of the ship, which is assumed to be 700 m^2 as investigating other similar size of container ships, $C_{D_{wind}}$ is wind drag coefficient from the chart of Blendermann (1994), which were determined by the regression of wind tunnel test data for a variety of ship types and sizes, and U_{wind} is wind speed.

Estimation for Ship Speed Loss

As described in Fig. 5, the total resistance (R_w) due to wind and wave can be estimated by adding the predicted calm water resistance (R_c) and the estimated results of the added resistance (ΔR_{wind} and ΔR_{wave}). The ship speed loss for each B.N. is predicted based on assumption that the required power at the reference ship speed in calm water is the same as the required power in the specific sea condition. In Fig. 5, P_{B_C} and P_{B_W} are the required brake power in calm water and the specific sea conditions, and V_c and V_w are the reference ship speed in clam water and achievable ship speed in the specific sea conditions at the same required brake power in calm water. Therefore, the ship speed loss can be obtained by subtracting V_w from V_c.

DISCUSSION OF RESULTS

In this section, the results of the motion responses, added resistance and ship speed loss estimations are presented by comparing with available experimental data and simulation results obtained by other researchers. The added resistance in ship motions is predicted in regular waves and the ship speed loss is estimated at assumed design and other lower speeds by the proposed methodology. They will be discussed separately in the following sections.

Added Resistance in Regular Waves

Prior to the investigation on the added resistance, motion transfer functions of heave and pitch are compared with the experimental data for validation because the added resistance due to waves is proportional to the relative motions (typically, heave and pitch motions) and inaccuracies in the predicted motions may amplify the errors in the added resistance. In this study, ξ_3, ξ_5 and A are the amplitudes of heave and pitch responses and incident wave respectively and $k = 2\pi/\lambda$ is the wave number in infinite depth seas. The heave and pitch motions are evaluated at the ship's centre of gravity. Fig. 6 shows the results of the heave transfer function comparing the results of present 2-D linear potential method and CFD with experimental data (Fonseca et al., 2004) in head seas at Fn=0.25 of the ship speed. The calculation results of the 2-D potential flow agree reasonably well with the experimental data except around peak value even though the heave motion is more difficult to predict accurately than the pitch motions (Bunnik et al. 2010). The success of the 2-D method is attributed to the high encountering frequencies. As it was explained before that the 2-D method assumes low Froude number, high frequency and slender body approaches in the Boundary Value Problem (BVP) solutions. Although the forward speed is high in the present problem, motion responses agreed well with the experimental results because the motions responses are mainly governed by the Froude–Krylov and restoring forces.

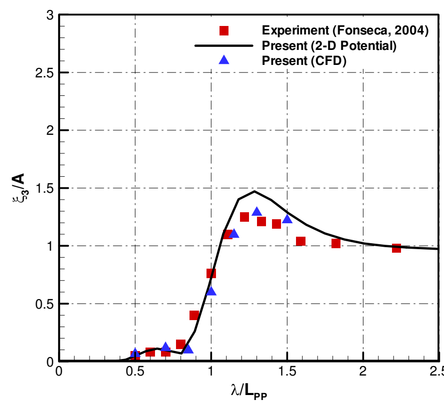

Fig. 6. Heave transfer function (Fn=0.25, θ=180°)

Fig. 7 presents the comparison result of pitch transfer function which indicates that both methods show good agreement with experimental data.

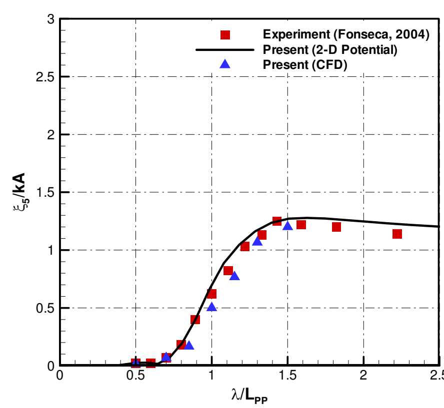

Fig. 7. Pitch transfer function (Fn=0.25, θ=180°)

The numerical results of the added resistance are compared with the available experimental data (Fujii and Takahashi, 1975; Nakamura et al., 1977) as illustrated in Fig. 8 which indicates that the numerical results are in agreement with the experimental data. In short waves where the hydrodynamic nonlinear effects are intensified (Kashiwagi et al., 2009), CFD method estimated the added resistance slightly better than the 2-D method but the results by both methods are similar because the present 2-D method is using the asymptotic method in short waves.

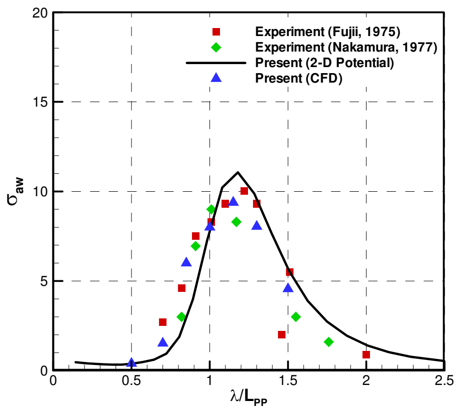

Fig. 8. Added resistance in Head Seas (Fn=0.25, θ=180°)

In addition to the calculation of the added resistance in head waves, validation studies on the added resistance for other wave heading angles to extend a study on the speed loss estimation due to irregular waves by 2-D potential method are performed by comparing with experimental results by Fujii and Takahashi (1975) as shown in Fig. 9.

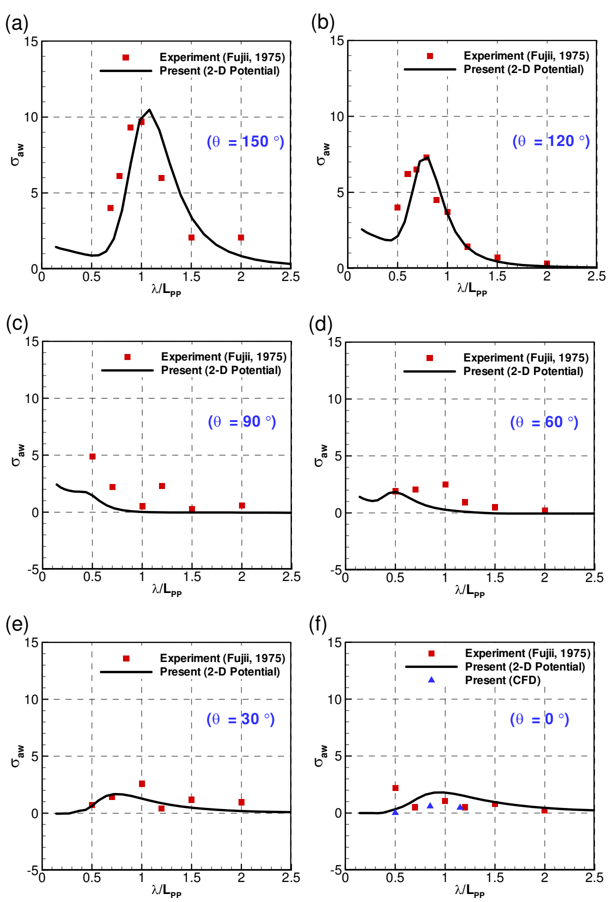

Fig. 9. Added resistance with varying wave heading (Fn=0.25)

Similar to head seas, the results for other wave heading directions showed similar trends using the 2-D method compared to the experimental data. For the following waves (Fig. 9(f)), the calculation of the added resistance was performed additionally by CFD, which is in reasonable agreement with the experimental results. Overestimation of the 2-D method is caused by the strip theory which provides poor results in low encountering frequencies and in high vessel speed, which will be confirmed by 3-D potential method or CFD as future studies.

Speed Loss Estimation in Random Seas

Based on the procedure of the developed approach, the speed loss due to wind and waves in random seas for S175 containership is estimated and compared with the available simulations performed by other researchers. The Kwon's method (2008) is based on semi-empirical model considering wind, motions and diffraction resistance, and the other study on the ship speed loss and CO_2 emission is based on ITTC spectrum by Prpić-Oršić and Faltinsen (2012) considering along with the propeller performance in actual sea. V_c is determined to be 23 kts (Fn=0.286) assuming the design speed of the vessel. Fig. 10 shows the estimated ship speed loss due to waves only and both wind and waves by the proposed approach. If the effect of only waves is considered, the speed loss estimated in head sea by the present approach is similar to the simulation results obtained by Prpić-Oršić and Faltinsen as shown in Fig. 10. Regarding the comparison with the results predicted by Kwon's method taking into account the effect of both wind and waves, the ship speed loss predicted by the present approach is less than the simulation results based on Kwon's semi-empirical model. But unlike the Kwon's method which predict the ship speed loss only in relation to B.N. without consideration of hull form, the developed methodology is able to estimate the ship speed loss with motions reflecting the hull form at the specific wave conditions of the height, frequency and direction and wind conditions of speed and direction separately as well as B.N.

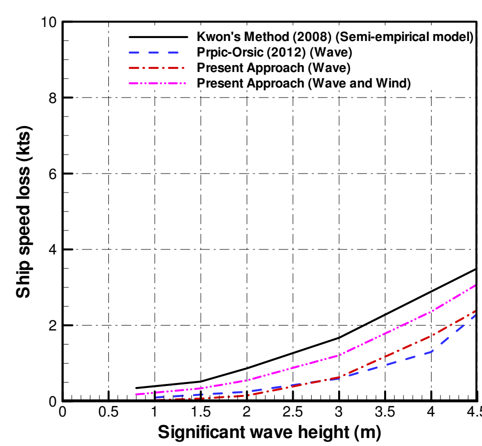

Fig. 10. Estimated ship speed loss due to wind and wave (Vc=23 kts)

The achievable ship speed due to waves and both wind and waves with weather direction under the assumption that the directions of wind and waves are collinear is estimated at B.N. 6 as the representative sea conditions as shown in Fig. 11. If the effect of both wind and waves are considered, the speed loss for the head and head quartering seas (θ=150°- 120°) is higher than the speed loss for the beam (θ=120°- 60°) and following seas (θ=60°- 0°). For the following sea, the speed loss is less than 0.2 kts because wind contributes towards the ship thrust. From the study on the speed loss at varying directions of wind and waves, the speed loss can be estimated with the ship operating direction relative to weather direction.

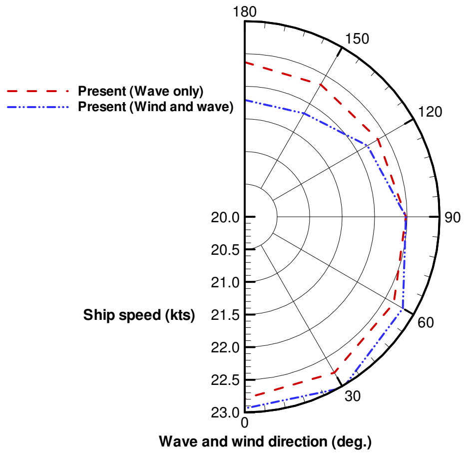

Fig. 11. Predicted ship speed with weather direction (Vc=23 kts, B.N.6)

Estimation of Ship Speed Loss and Sea Margin

The speed of a vessel has a dramatic impact on the fuel consumption because the speed is related to the propulsive power required exponentially. This significant savings make it easy to understand why there is substantial interest in slow steaming, especially when fuel prices escalate. The effect of the ship speed loss at other lower speeds was investigated taking account of the slow steaming of the containership speeds. With the estimation of ship speed loss due to wind and irregular waves respectively, sea margin of the ship at the representative sea conditions of B.N.6 is also estimated based on the proposed methodology for lower ship speeds (V_c = 20.14 and 16.11 kts) including the design speed (V_c=23 kts) in calm water. It is summarized in Table 4 that as the ship reference or operating speed is decreased, the ship speed loss is higher and hence higher sea margin is needed to achieve the same reference ship speed at the sea conditions of B.N.6 in head seas. Ship speed reduction due to wind and waves based on the variation of the reference speed from 23 kts to 16.11 kts are 0.2 kts and 0.42 kts respectively, hence the effect of the decrease in ship speed in the speed loss due to waves is higher than wind. Furthermore, the sea margin is increased despite the decrease in the absolute value of the required additional power (e.g. 5.5% increase for the speed change from 23 kts to 16.14kts but 11.7% increase for the speed change from 20.14 kts to 16.11 kts).

Table 4. Predicted speed loss and sea margin (B.N.6, θ=180°)

Ship speed	23 kts (Fn = 0.286)	20.14 kts (Fn = 0.25)	16.11 kts (Fn = 0.20)
Total speed loss due to wind and waves	1.21 kts	1.33 kts	1.83 kts
Speed loss due to wind	0.58 kts	0.63 kts	0.78 kts
Speed loss due to waves	0.63 kts	0.70 kts	1.05 kts
Sea margin	17.2 %	22.7 %	34.4 %

CONCLUSIONS

A reliable methodology to estimate the added resistance and ship speed loss of S175 containership due to wind and waves is proposed depending on the specific wind and wave conditions corresponding to each Beaufort scale. The reduction of the ship speed in realistic sea conditions was investigated in detail using the developed approach and is compared with simulation results predicted by other researchers, which shows that the proposed approach can be used to predict the ship speed loss taking account of actual sea conditions on ship operation. From the estimated results of the ship speed loss due to wind and waves, at low B.N., the effect of wind on the ship speed loss is observed to be higher than wave but, at high B.N., which means that the sea condition is getting severe, the speed loss due to wave is bigger than that due to wind. At the representative sea conditions at B.N. 6, the speed losses due to only wind and both wind and waves are predicted with respect to weather direction. From the study on the speed loss at varied directions of wind and waves, the speed loss can be estimated with the ship operating direction relative to weather direction.

The proposed methodology is developed considering latest IMO and ITTC guideline/ recommendation. Therefore, this study will be helpful for the calculation of fw in the EEDI formulation and the assessment of the environmental impact. Also, with ship main particulars and hull form lines even in the ship design stage, it is possible to design the hull form with better performance not only in calm water but also in a seaway considering the speed loss and ship motions which are related to the ship safety in her operation. In the developed approach, the prediction methods for the added resistance can be changed (e.g. wind tunnel test results of the ship instead of Blendermann chart as general empirical chart for the prediction of the added resistance due to wind).

Before predicting the added resistance and ship speed loss due to wind and irregular waves, wide range of validation studies are performed for the added resistance with ship motions in regular head and oblique seas using the 2-D linear potential theory and URANS simulations by CFD. From validation studies for the motions of heave and pitch and the added resistance, the characteristics of 2-D linear potential method and CFD were investigated and numerical results agree reasonably well with the experimental data in regular head and oblique seas, which indicates that the 2-D method can be extended to calculate added resistance for the ship in irregular waves to save computational time and costs. For the following seas, the added resistance was calculated additionally by CFD, which also shows reasonable agreement with 2-D potential method result and experimental data.

Finally for other two lower speeds (V_c = 20.14 and 16.11 kts) including the assumed ship design speed (V_c=23 kts) at head weather, changes in the ship speed and required sea margin due to wind and waves to achieve the initial reference speed (V_c) have been investigated at B.N.6 which was adopted by MEPC with the representative sea conditions. This study indicates that as the ship operating speed is decreased, total speed loss due to both wind and waves is getting larger, especially due to waves. It should be noted that if a ship operator would order to reduce the ship speed, the difference between the ordered speed and the actual ship speed is getting larger at the same wind and wave conditions in a seaway. Also, the estimated sea margin is significantly increased when the initial reference speed is decreased even though the absolute value of the required additional power is reduced.

FUTURE WORKS

Continuous study on the added resistance with ship motions for other ship types such as tankers and bulkers as blunt hulls and further development of a reliable methodology to estimate the ship speed loss in a seaway will be carried out by using other approaches, especially 3-D potential theory.

ACKNOWLEDGEMENTS

This research has been funded by the Engineering and Physical Research Council (EPSRC) through the project, “Shipping in Changing Climates. All supports are greatly appreciated. EPSRC grant no. EP/K039253/1.
It is noted that the results were obtained using the EPSRC funded ARCHIE-WeSt High Performance Computer (www.archie-west.ac.uk). EPSRC grant no. EP/K000586/1.

REFERENCES

Arribas, F. P. (2007). “Some methods to obtain the added resistance of a ship advancing waves,” *Ocean Engineering*, 34, 946-955.

Banks, C., Turan, O., Incecik, A., Theotokatos, G., Izkan, S., Shewell, C., Tian, X. (2013). “Understanding ship operating profiles with an aim to improve energy efficient ship operations,” *In: Proceedings of the Low Carbon Shipping Conference*, London, 1–11.

Blendermann, W. (1994). “Parameter identification of wind loads on ship,” *Journal of Wind engineering and Industrial aerodynamics*, 51, 339-351.

Boese, P. (1970). “Eine einfache Methode zur Berechnung der Widerstanderhöhung eines Schiffes im Seegang,” *Journal Schiffstechnik-Ship Technology Research*, 17 (86).

Bunnik, T., Daalen, R.V., Kapsenberg, G., Shin, Y., Huijsmans, R., Deng, G., Delhommeau, G., Kashiwagi, M., and Beck, B. (2010). “A comparative study on state-of-the-art prediction tools for seakeeping,” *In: Proceedings of the 28th Symposium on Naval Hydrodynamics*, USA, 1-13.

Faltinsen, O.M., Minsaas, K.J., Liapis, N., and Skjørdal, S.O. (1980). “Prediction of resistance and propulsion and propulsion of a ship in a seaway,” *Proceeding of 13th Sym. Naval Hydrodynamics*, Tokyo, 505-529.

Fonseca, N. and Guedes Soares, C. (2004). “Experimental investigation of the nonlinear effect on the vertical ship motions and loads of a containership in regular waves,” *Journal of Ship Research*, 48(2), 118-147.

Fujii, H. and Takahashi, T. (1975). “Experimental study on the resistance increase of a ship in regular oblique waves,” *Proceeding of 14th ITTC*, Ottwa, 351-360.

Gerritsma, J. and Beukelman, W. (1972). “Analysis of the resistance increase in waves in a fast cargo ship,” *Intern. Shipbuilding Progr.* 19(217), 285-93.

Guo, B.J., Steen, S. and Deng, G.B. (2012) Seakeeping prediction of KVLCC2 in head waves with RANS, Appl. Ocean Res., 35, 55-67.

Havelock, T.H. (1937). “The resistance of a ship among waves,” *Proc. Roy. Soc*. London A, 161, 299-308.

Holtrop, J.A. and Mennen, G.G.J. (1978). “A statistical power prediction method,” *International Shipbuilding Progress*.

Holtrop, J.A. and Mennen, G.G.J. (1982). “An Approximate Power Prediction Method,” *International Shipbuilding Progress*, Amsterdam.

Holtrop, J.A. (1984). “Statistical Reanalysis of Resistance and Propulsion Data,” *International Shipbuilding Progress*, Amsterdam.

International Maritime Organisation (IMO) (2012). “Interim guidelines for the calculation of the coefficient fw for decrease in ship speed in a representative sea condition for trial use,” MEPC.1/Circ.796.

International Towing Tank Conference (ITTC) (2014). “The specialist committee on seakeeping-final report and recommendations to the 27th ITTC,” Copenhagen.

Joncquez, S.A.G. (2009). “Second-order forces and moments acting on ships in waves,” *Ph.D. thesis*, Technical University of Denmark.

Joosen, W.P.A. (1966). “Added resistance of ships in waves,” *Proc. 6th Symp. Naval Hydrodynamics*, Wasington, D.C.

Kashiwagi, M. (2009). “Impact on hull design on the added resistance in waves - application of the enhanced unified theory,” *In: Proceedings of the 10th International Marine Design Conference (IMDC)*, Trondheim, Norway, 521-535.

Kashiwagi M., Ikeda T. and Sasagawa T. (2009). “Effects of forward speed of a ship on added resistance in waves,” *In: Proceedings of the 19th International Offshore and Polar Engineering Conference*, Osaka, Japan, ISOPE, 3, 818-825.

Kim, H.T., Hong, C.B., Lee, G.H., Kim, and B.K. (2015). “Prediction of added resistance of a ship in waves using computational fluid dynamics,” *In: Proceedings of the Annual Spring Conference*, SNAK, Korea, 465-478.

Kim, H.T., Kim, J.J., Choi, N.Y., Lee, and G.H. (2014). “A study on the operating trim, shallow water and wave effect,” *In: Proceedings of the Annual Autumn Conference*, SNAK, Korea, 631–637.

Kim, K.H., Kim Y., and Kim, Y. (2007). “WISH JIP project report and manual”, Marine Hydrodynamic Laboratory, Seoul University.

Kim, K.H., Seo, M.G., and Kim Y.H. (2012). “Numerical analysis on added resistance of ships,” *International Journal of Offshore and Polar Engineering,* ISOPE, 22, 21-29.

Kim, M.G. and Park, D.W. (2015). “A study on the green ship design for ultra large container ship,” *Journal of the Korean Society of Marine Environment & Safety*, 21, No. 5.

Kwon, Y.J. (2008). “Speed loss due to added resistance in wind and waves,” *the Naval Architect* 3, 14-16.

Loukakis, T.A. and Sclavounos, P.S. (1978). “Some extensions of the classical approach to strip theory of ship motions, including the calculation of mean added forces and moments,” *Journal of Ship Research*, 22, 1-19.

Maruo, H. (1960). “The drift of a body floating on waves,” *Journal of Ship Research*, 4(3), 1-10.

McTaggart, K., Datta, I., Stirling, A., Gibson, S., and Glen, I. (1997). “Motions and Loads of a Hydroelastic Frigate Model in Severe Seas,” *Society of Naval Architects and Marine Engineers* 105.

Nakamura, S. and Naito, S. (1977). “Propulsive performance of containership in waves,” *Journal of Soc. Naval Architect. Japan*, 15, 24-48.

Newman, J.N. (1967). “The drift force and moment on ships in waves,” *Journal of Ship Research*, 11, 51-60.

Open University (1999). “Waves, Tides and Shallow Water Processes,” second edition, Butterworth-Heinemann, Oxford.

Park, D.M., Seo, M.G., Lee, J.H., Yang, K.K., and Kim, Y.H. (2014). “Systematic experimental and numerical analysis on added resistance in waves,” *Journal of the Society of Naval Architects of Korea*.

Prpić-Oršić, J. and Faltinsen, O.M. (2012). “Estimation of ship speed loss and associated CO2 emissions in a seaway,” *Ocean Engineering* 44, 1-10.

Sadat-Hosseini H, Wu P, Carrica P.M., Kim H, Toda Y, and Stern F. (2013). “CFD verification and validation of added resistance and motions of KVLCC2 with fixed and free surge in short and long head waves,” *Ocean Engineering*, 48, 240-273.

Salvesen, N., Tuck, E.O., and Faltinsen, O.M. (1970). “Ship motions and sea loads,” *SNAME*, Jersey City.

Simonsen, C., Otzen, J., Joncquez, S., and Stern, F. (2013). “EFD and CFD for KCS heaving and pitching in regular head waves,” *J Mar Sci Technol.*, 18, 435-459.

Tezdogan, T., Demirel, Y.K., Kellett, P, Khorasanchi, M., and Incecik, A. (2015). “Full-scale unsteady RANS CFD simulations of ship behaviour and performance in head seas due to slow steaming,” *Ocean Engineering*, 97, 186-206.